Crashworthiness Design for an Electric City Car against Side Pole Impact

Rachman Setiawan* **& Mohammad Rusyad Salim**

Faculty of Mechanical and Aerospace Engineering, Institut Teknologi Bandung
Jalan Ganesha No. 19, Bandung 40132, Indonesia
*E-mail: rachmans@edc.ms.itb.ac.id

Abstract. Electric vehicles are increasingly popular as an alternative to fossil fuel vehicles. The presence of batteries and electric motors poses different risks in collision accidents. The deformation of the batteries could spark a fire or explosion that in turn could endanger the passengers. The prototype of an Indonesian electric city car is currently being developed, which includes a battery pack located underneath the passenger compartment and electric motors in the front compartment. A crashworthiness design against side pole impact, in accordance with the Euro NCAP standard, was simulated numerically. In order to reduce the risk of battery explosion, an impact energy absorbing structure is proposed for implementation at the sides of the batteries. The structure of the four-passenger hatchback electric city car was modeled using all-shell elements with material properties for common automotive application and analyzed using the finite element method with dynamic plasticity capability. For the preliminary design, the minimum deformation of the batteries that can cause battery explosion was used as the failure criteria. From a number of design alternatives, the use of aluminum foam as impact energy absorber produced sufficient protection for the battery pack against side pole impact, hence effectively reducing the risk to an acceptable limit.

Keywords: *battery deformation; crashworthiness; electric vehicle; impact absorber; NCAP; side pole impact.*

1 Introduction

In the future, electric vehicles are expected to play an important role in traffic, replacing conventional fossil fuel vehicles in view of energy and environmental issues. Electric vehicles, including plug-in hybrid electric vehicles (PHEV), range extender battery electric vehicles (RE BEV) and pure battery electric vehicles (BEV), consist of three important components, namely batteries that provide energy, an electric motor that drives the wheels, and a controller that regulates the energy flow to the motor. Currently, the automotive industry is mostly interested in lithium ion battery technology since it provides one of the best energy densities at a rational price available today [1,2]. As energy storage with high energy density, lithium ion batteries face some challenges in both functional safety and crash safety.

Received July 25th, 2017, Revised October 23rd, 2017, Accepted for publication November 6th, 2017.
 ISSN: 2337-5779, DOI: 10.5614/j.eng.technol.sci.2017.49.5.3

Standard lithium ion battery cells consist of stacked or wrapped layers of anodes and cathodes, which are physically separated by a porous but mechanically robust separator foil. This separator prevents the battery from internal short circuiting. A severe accident that causes enough battery deformation may damage the separator, causing internal short circuiting to occur. This event will make the temperature of the battery cell increase rapidly. Its high energy density makes it worse, as the whole battery will reach a very high temperature and may initiate a fire. A case of a fire accident has occurred recently when a car crashed with metal debris on the highway, causing the car battery to deform and the battery cell temperature to rise suddenly. As a consequence, the battery exploded, as can be seen in Figure 1. In order to avoid such an event, the mechanical deformation of lithium-ion battery cells must be prevented from exceeding a certain limit. This deformation and the related electro-mechanical failure have been studied, among others, by Greve and Fehrenbach [3]. In their study, cylindrical lithium ion cells were subjected to various mechanical abuse tests in order to create a crash simulation model of the cells. The developed simulation model allows the representation of cell deformation and also features a stress-based fracture criterion for predicting the load state and location for internal short circuiting onset during deformation.

Figure 1 A case of a battery fire accident due to collision [4].

On the other hand, the need for long distance travel requires a larger battery pack in electric vehicles, which must be wisely integrated in the vehicle body structure. There are at least two design concepts for battery packs, namely the 'T' architecture and the 'floor' architecture (see Figure 2). The 'T' architecture offers excellent protection against both frontal collision and side impact but is not optimal in terms of comfort and interior spaciousness. The 'floor' architecture has a lower center of gravity and leaves the entire interior space clear, which is suitable for a city car, which already has a small body. The disadvantage of this configuration is the susceptability to side impacts.

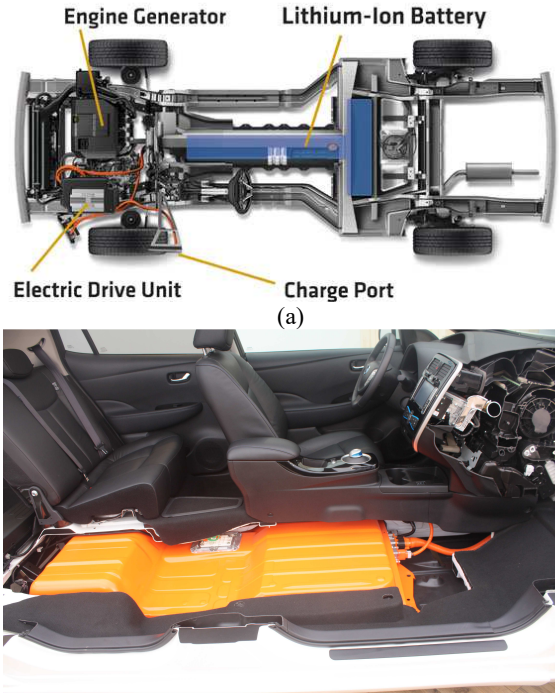

Figure 2 Battery pack locations: (a) 'T' configuration in Chevrolet Volt [5], (b) 'floor' architecture in Nissan Leaf [6].

The Euro New Car Assessment Program (Euro NCAP) has two tests to assess the ability of a vehicle to provide safety during side impacts. The first test, which is called the Side Impact Mobile Deformable Barrier, uses a trolley with a deformable barrier, which is launched into a stationary test vehicle and impacts the car's centerline at 33.5 mph (50 km/h) [7]. The barrier consists of an aluminum honeycomb bumper that is mounted on an aluminum honeycomb block, which impacts a large portion of the vehicle's side from the front to the rear wheel area. This test simulates the impact to the side of a vehicle from another vehicle. The forces and accelerations on anthropomorphic test dummies are the focus of this test. The second test, which is called the Oblique Side Pole Impact Test, uses a 10" (254 mm) fixed rigid pole as the impacted object [8]. The vehicle is launched to the centerline of the pole at 20 mph (32.2 km/h) at an angle of 75° to the longitudinal axis of the vehicle and through the center of gravity of the dummy driver's head. This test simulates a vehicle that crashes into a fixed utility pole or tree. Both tests are illustrated in Figure 3.

In this study, a preliminary crashworthiness design was developed as part of an attempt to develop an Indonesian electric car. The pure battery electric car being developed is a small 4-passenger city car. As common in the design of small electric vehicles, the battery pack is placed underneath the passenger compartment, hence it is prone to side impacts. Therefore, in this investigation the Oblique Side Pole Impact Test was used because it is expected to introduce higher deformation on the vehicle floor and poses a direct threat of battery fire or explosion. This study used LS-DYNA, a finite element based software analysis with dynamic plasticity modeling capability with explicit time integration for the simulation of crash-testing.

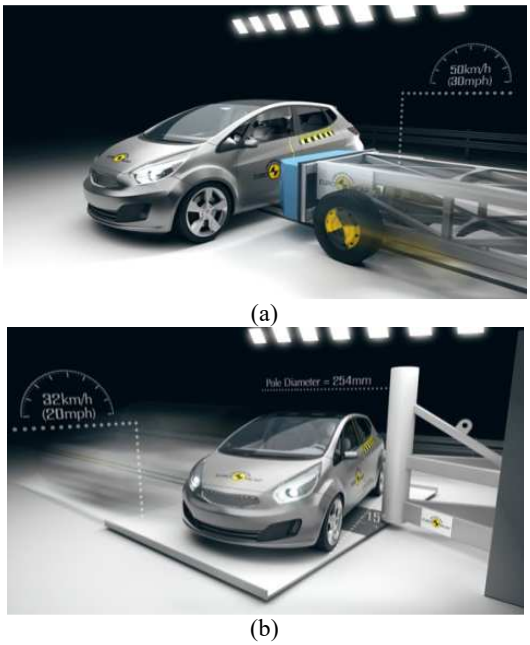

(a)

(b)

Figure 3 Illustration of side impact tests [9]: (a) Side Impact Mobile Deformable Barrier, (b) Oblique Side Pole Impact Test.

A number of design alternatives to avoid or reduce deformation of the batteries and hence reduce the risk of fire were explored. The idea is to fill the door sill area, instead of the door or the roofline, with a number of alternative impact absorbers, in order to maximize the available space. For the preliminary design, the minimum deformation of the batteries that can cause battery explosion was used as the failure criteria. This study compared three alternative impact absorbers for filling the door sill, i.e. a simple hollow cylinder structure (conventional), aluminum honeycomb, and aluminum foam.

2 Simulation

2.1 Finite Element Model

2.1.1 Geometry

Here, the geometry of the whole car, complete with body, chassis, doors and other components related to the integrity of the side structure of the car, was modeled as closely as possible to the actual components. Other components that are not related to the integrity of the car's side structure, such as the electric motors, wheels, dashboard and luggage door, were simplified as rigid structures with accurate information of mass and center of gravity, since these aspects affect the inertia forces but not the integrity of the structure during collision. The surface geometry of the whole car can be seen in Figure 4.

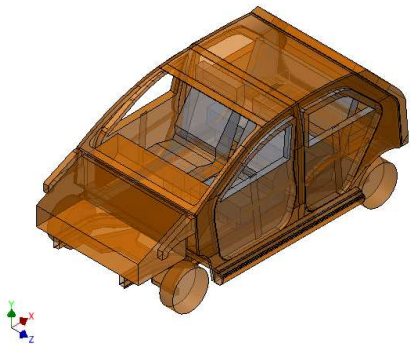

Figure 4 Surface geometry model of the electric city car.

The battery geometry used in this paper refers to that of a Mitsubishi i-Miev electric car [10]. The battery modules are distributed underneath the passenger seats, both in the front and the rear, as shown in Figure 5(a). The same configuration was adopted in the design of the electric car currently under development, as can be seen in Figure 5(b).

The impact absorber was designed to be placed inside the door sill. The battery pack itself was also equipped with a side impact channel structure. The following three alternative impact absorbers were considered:

1. Hollow aluminum cylinders, with 1.5" diameter (OD = 48.26 mm) and 146 mm height. They were modeled in the finite element software as shells of isotropic material.

2. Aluminum honeycomb, with dimensions as shown in Figure 6 and characteristics as specified in Paik, *et al* [11]. It was modeled in the finite element software as a solid of anisotropic material.
3. Aluminum foam, with characteristics as specified in Yu and Banhart [12]. It was modelled in the finite element software as a solid of isotropic material.

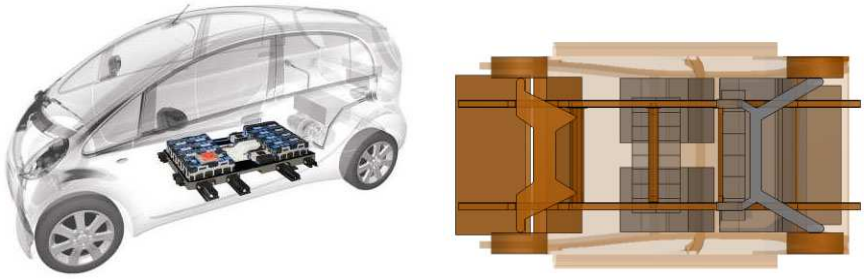

(a) (b)

Figure 5 Battery module placement: a) in the Mitsubishi i-Miev [10], b) in the car under development.

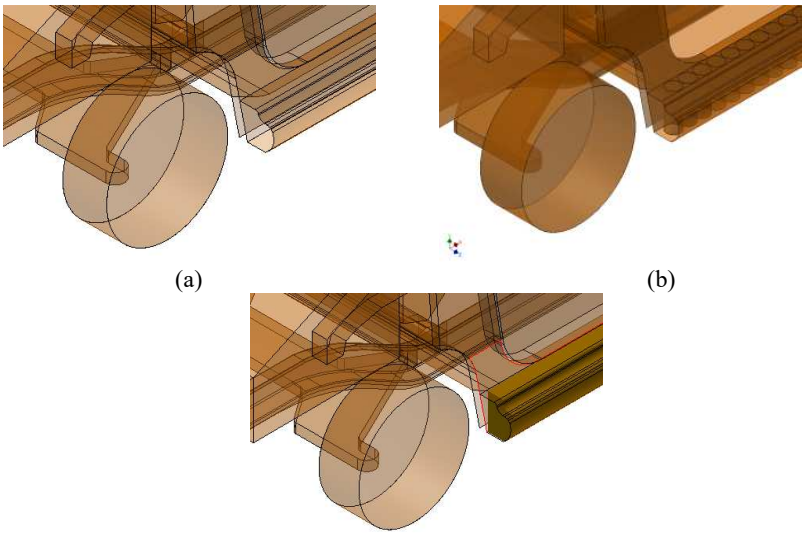

(a) (b)

(c)

Figure 6 Details of design alternatives in the model: a) hollow structure only, b) lateral cylinder, c) aluminum honeycomb or foam.

Figure 7 shows the placement of the three design alternatives in the model. The honeycomb and foam were made using the solid feature with dimensions adjusted to the door sill geometry.

2.1.2 Materials

Side crash test simulations involve many components of various materials. Selection of the right material in this simulation was very important in order to approach the actual conditions. In general, the mechanical properties of the materials that need to be known are strength, stiffness, density, modulus of elasticity, and Poisson's ratio, and if possible the stress–strain curve. Four types of materials were used in this simulation, as shown in Table 1.

Table 1 Mechanical properties of materials.

Material	SPHC[1]	Al 3102-O[2]	Al honeycomb[3]	AlSi foam
Density (kg/m^3)	7,870	2,710	54.4	390
Young's modulus (GPa)	218	70	0.54[3], 0.054[4]	0.175
Poisson's ratio	0.3	0.33	0.05	0.05
Yield stress (MPa)	436	30	2.17[3], 0.217[4]	
Tensile strength (MPa)	674	95		
Elongation	19%	40%		

Notes:
[1] for Chassis, body, and battery case
[2] for hollow pipe
[3] direction and dimensions as illustrated in Figure 6(a).

The mechanical properties of the SPHC were extracted from material testing conducted by the authors, while those of the aluminum honeycomb and foam were obtained from Paik, *et al.* [11] and Yu, *et al.* [12], respectively. The geometries of the honeycomb-core and aluminium foam were found from their respective references, as shown in **Error! Reference source not found.**.

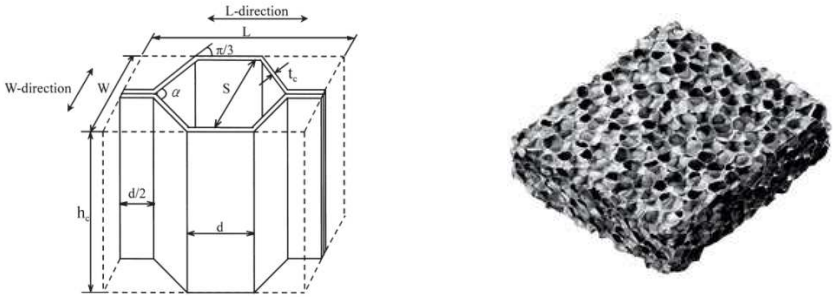

(a) (b)

Figure 7 Material to be used as alternative impact absorbers: (a) honeycomb-core unit [11], (b) aluminum foam [12].

This study used five different keywords to define the material properties, namely MAT 20 RIGID (for rigid components), MAT 24

PIECEWISE_LINEAR_ PLASTICITY (for chassis, body and cylinder hollow), MAT 26 Honeycomb (for honeycomb), and MAT 063 CRUSHABLE_FOAM (for metallic foam), available in the LS-Dyna package software.

2.1.3 Discretization

The geometric model was then meshed with the material properties as inputted according to Table 1, initially using the default size specified in the software. For components modeled as rigid elements, such as electric the motors and wheels, the size was 50 to 100. The final meshed model of the car can be seen in Figure 8 while the model of the impact-absorbing module is shown in Figure 9.

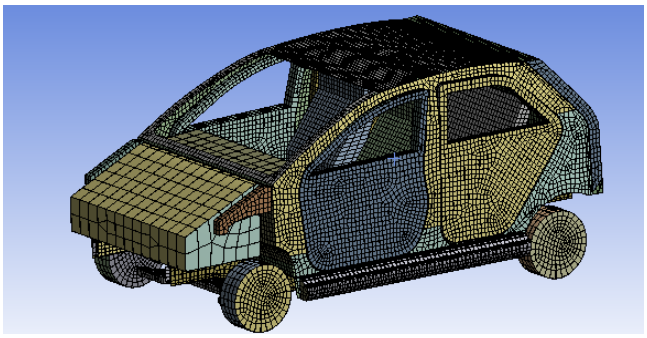

Figure 8 Finite element model of entire car.

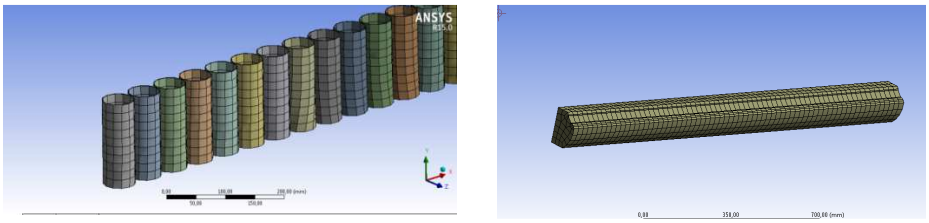

(a) (b)

Figure 9 Discretization of impact absorber module: (a) hollow cylinder, (b) honeycomb or foam.

Shell elements were used for most of the car's parts, except the honeycomb and foam. These shell elements use standard calculation formulation types, namely Belytschko-Tsay, with a quadrilateral and triangular shape. The honeycomb and foam were modeled with solid elements that are compatible with the modeling strategy of such materials. Finally, the completed model without impact absorber contained approximately 47,771 elements and 50,507 nodes.

2.1.4 Contact Model

Two different contact algorithms were used. The contact among the parts were modeled with automatic single surface contact, with friction coefficient of 0.74. Another contact type that was used in this simulation was automatic surface-to-surface tiebreak. For tied contacts without offset option, any slave nodes that meet the criteria for tying were moved to the master surface during initialization, thus eliminating gaps between slave nodes and master segments.

2.1.5 Boundary Conditions

The function of the boundary conditions is to create and define constraints and loads on the finite element model. For the Oblique Pole Side Impact Test, a rigid pole with fixed boundary condition was defined, i.e. constrained in either translation or rotation on the *x*, *y*, and *z*-axes. The whole vehicle was then moved with an initial velocity of 20 mph (approximately 8.9 m/s) before it impacted the wall.

2.1.6 Mass Loading

The mass data for each primary car components can be seen in Table 2. The data were based on the actual components as well assumptions based on a similar-sized car, such as the Mitsubishi i-Miev or the Kia Picanto.

Table 2 Mass data of components.

Component/part	Mass (kg)
Driver seat	13
Front passenger seat	13
Back seat	29
Front compartment	180 + 9
Dashboard	10
Battery	212
4 wheel + brake + suspension	4 × (13 + 17 + 4)
Front subrame + arm	30 + 7
Rear subframe	20
Chassis	50
Body	150
4 doors	4 × 18
Luggage door	17
Others	220
Dummy	75
Luggage mass	68
Total	**1310**

2.1.7 Time Termination

The time value of the termination-input in this simulation was set to 80 ms. This value was obtained by looking at the curve of the kinetic energy and the internal energy simulation results. When the kinetic energy and internal energy reached steady state condition, the impact energy was depleted and the simulation was terminated.

2.1.8 Time Step and Hourglass

The time step used in a finite element simulation should not be greater than the critical time step. In this investigation, the default time-step value was used, while large time step was set to 90% of the critical time step. The critical time step was calculated automatically by the software.

Hourglass modes are nonphysical, zero-energy modes of deformation that produce zero strain and no stress. Hourglass modes occur only in under-integrated (single integration point) solid, shell, and thick shell elements. LS-DYNA has various algorithms for inhibiting hourglass modes. In this simulation, the value of hourglass was set to the default value, i.e. 0.1.

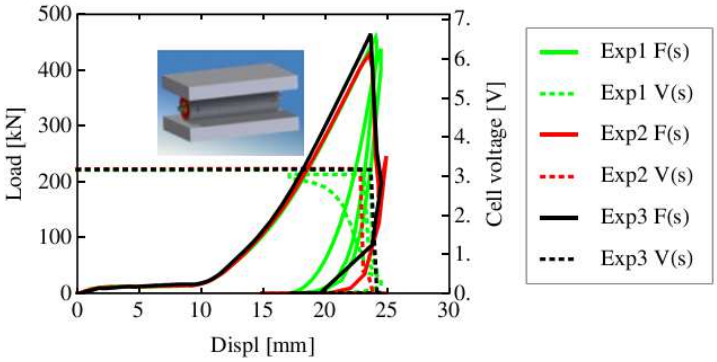

Figure 10 Experimentally obtained punch load–displacement and cell voltage curves [3].

2.2 Failure Criteria

This section contains a discussion of the failure criteria of the battery. In a battery there are two active materials, i.e. the anodes and the cathodes, whereby both materials are separated by a separator. The separator serves to prevent contact between the anode and the cathode. A severe accident that causes enough battery deformation can damage the separator, resulting in internal short circuiting, which in turn can initiate a battery fire or explosion. According to

Greve and Fehrenbach [3], the smallest displacement that can cause battery failure is approximately 23 mm. During the design stage, a safety factor of 1.5 was used so that the limit of mechanical deformation on the battery was 15.3 mm, as can be seen in Figure 10. This limit was used as the failure criteria in the comparison of the three alternative impact absorbers.

3 Result and Discussion

The crash test simulations were performed using four models, i.e. i) structure without impact absorber as baseline, ii) hollow cylinders, iii) aluminum honeycomb, and iv) aluminum foam. Besides the deformation as the main aspect of comparison, the amount of absorbed energy and mass were also compared. The former is used to check whether all impact energy has been absorbed, while the latter is used to estimate the additional mass to the vehicle.

3.1 Hollow Structure Only (No Impact Absorber)

Figure 11 shows the global energy curve that compares the different energies involved in the process of collision. The main governing energy is the kinetic energy, as occurs initially at 51.96 kJ, obtained from the input of mass and initial velocity of the vehicle. During the collision process this decreases when the internal (strain) energy increases while the door sill structure deforms. This deformation serves as energy absorption during the collision. The total energy serves as a control that should be constant as a consequence of the law of energy conservation. In the case of a hollow structure only (no impact absorber), after 80 ms of simulation the internal energy reached an asymptotic value of 43.09 kJ, while there is still some remaining kinetic energy left, resulting in the vehicle still moving.

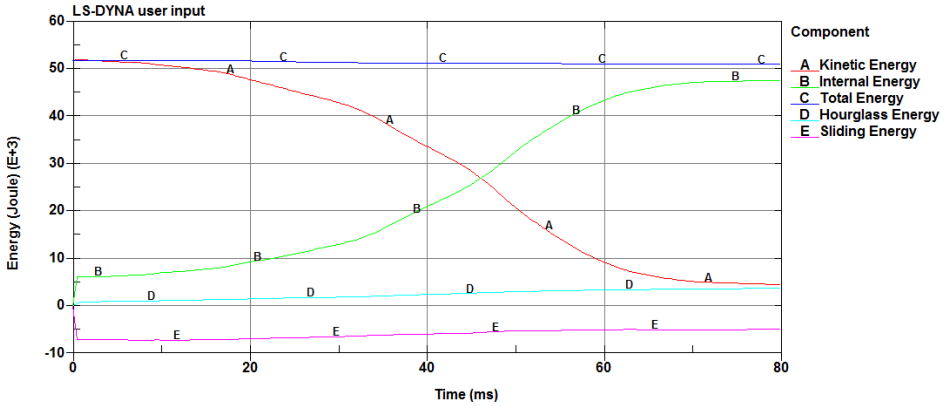

Figure 11 Global energy vs. time curves for the case of door sill without impact absorber.

The deformed shape of the car's structure can be seen in Figure 12. It shows that not all of the kinetic energy was absorbed by the structure. As a result, a portion of the energy will be transferred to the battery pack, as evidenced by a significant deformation of the protector of the batteries, as can be seen in Figure 13. From the simulation it was found that the maximum local deformation of the battery was 23.7 mm, thus exceeding the failure criteria limit of 15.3 mm. This indicates that the deformation of the battery was unacceptable.

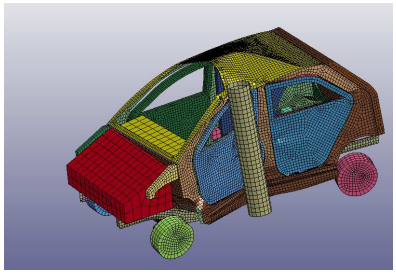

Figure 12 Deformation of the whole car's structure.

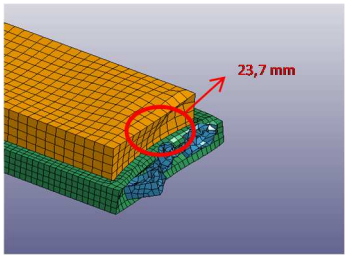

Figure 13 Deformation of battery and protector for the case of no impact absorber.

3.2 Structure with Hollow Pipes

In order to increase the crashworthiness, the door sill structure was filled with a deformable body as impact absorber. As the first design alternative, hollow cylinders were used in this simulation, consisting of 1.5" pipes with three different thicknesses, i.e. 3.68 mm (standard thickness), 5.08 mm (XS), and 10.16 mm (XXS). Figures 14 and 15 show the deformed shapes of the battery pack and the impact absorbers from the simulation, for each of the three thickness values. The energy absorbed in the case of the door sill filled with hollow pipes was 43.9, 44.0, 44.7 kJ for a pipe thickness of 3.68, 5.08 mm and 10.16 mm, respectively. There was a small addition in the absorbed energy with the presence of hollow pipes. The battery deformation was found to be 21.4,

19.7 and 21.6 mm for a pipe thickness of 3.68, 5.08, and 10.16 mm, respectively, all exceeding the failure criteria limit. Hence this solution must be considered unsafe. From the solid model it can be found that the additional masses were 14.6, 20.0, and 39.8 kg for a pipe thickness of 3.68, 5.08, and 10.16 mm, respectively.

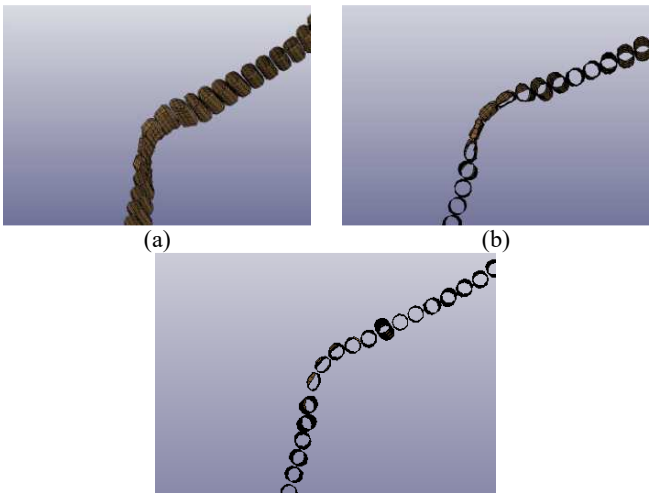

Figure 14 Deformation of hollow pipes with a thickness of a) 3.68 mm, b) 5.08 mm, c) 10.16 mm.

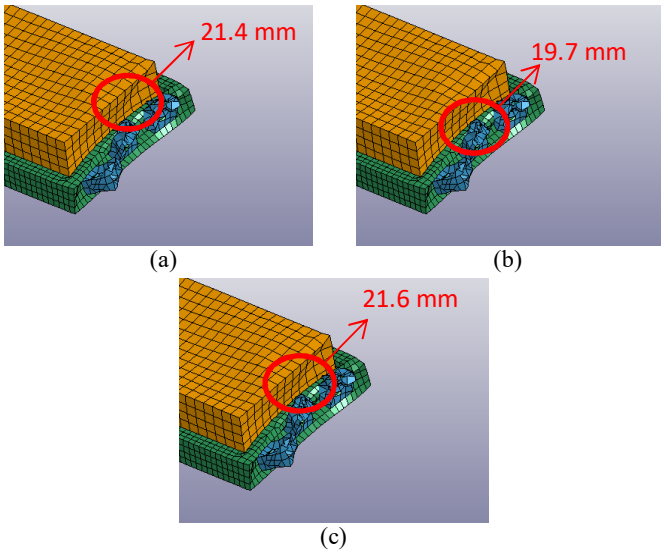

Figure 15 Deformation of battery and protector for hollow pipes with a thickness of a) 3.68 mm, b) 5.08 mm, c) 10.16 mm.

3.3 Aluminum Honeycomb

For the design alternative of the door sill being filled with an aluminum honeycomb structure, the additional mass was estimated at only 2.6 kg. The total energy absorbed with this alternative was 44.2 kJ. The deformed shape of the door sill filled with the honeycomb structure after the collision can be seen in Figure 16. Apart from global deformation, as in the door sill structure without impact absorber, internal deformation of the honeycomb structure occurred, though not significantly. The deformed shape of the batteries and its protector can be seen in Figure 17, with maximum deformation occurring in the battery equal to 18.9 mm, exceeding the failure criteria limit. From the deformed shape of the door sill it can be observed that the honeycomb produced less absorption due to the presence of more hollow spaces.

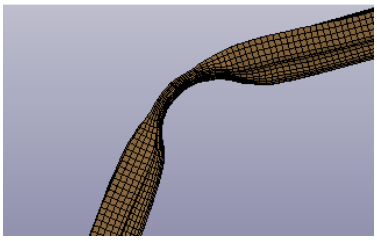

Figure 16 Deformation of aluminum honeycomb door sill.

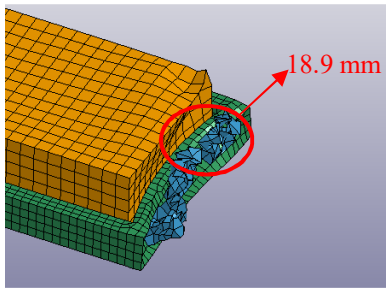

Figure 17 Deformation of battery pack in the case of aluminum honeycomb.

3.4 Aluminum Foam

The alternative of using aluminum foam produced 46.0 kJ of absorbed energy, the highest among the alternatives. From Figure 18, it can be observed that its deformation seems less than that of the aluminum honeycomb. However, in fact more deformation occurred inside the door sill structure due to the impact absorber. Since the foam structure was modeled as a solid, the detail deformation cannot be observed. As a result, a maximum deformation of 9.4

mm was produced in the battery pack, the smallest among the alternatives, as can be seen in Figure 19. This deformation is within the failure criteria limit. With its higher density of the deformable body, this alternative can absorb more energy, hence transferring less impact energy to the battery pack and producing less deformation of the battery pack. However, it also gave a high additional mass of 18.8 kg, which is unlikely to be applied in a small city car.

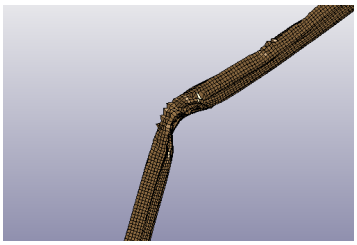

Figure 18 Deformation of aluminum foam door sill.

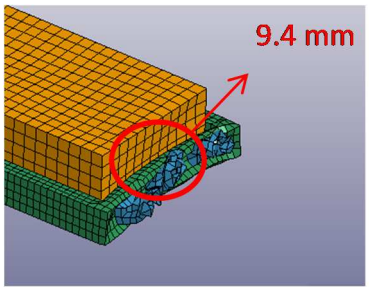

Figure 19 Deformation of battery pack in the case of aluminum foam.

3.5 Summary

Table 3 summarizes the results of the simulations. Among all alternatives, only that of using aluminum foam as the filler for the door sill structure gave a battery pack deformation that is acceptable, i.e. 9.4 mm compared to the 15.3 mm limit. From the trial of several alternatives it is possible to see the direction of further improvement. The key to an optimum design, i.e. high impact energy absorption and low additional mass, is to find a suitable density of the aluminum foam. The same could also apply in the case of using a honeycomb structure or hollow pipes, resulting in optimum sizes and numbers of components. Here, only steel and aluminum were considered as materials. While steel produces high additional mass, for the application in a small city car aluminum is preferrable, which produces a relatively low additional mass. Another consideration is manufacturability. Among the considered alternatives, the hollow pipe alternative is considered the easiest to acquire and assemble.

Table 3 Result summary.

Alternatives	Absorbed Energy (kJ)	Maximum Battery Deformation (mm)	Additional Mass (kg)
No impact absorbers	43.1	23.7	0
Hollow pipes (XS)	44.0	19.7	20.0
Al honeycomb	44.2	18.9	2.6
Al foam	46.0	9.4	18.8

4 Conclusion

From the numerical investigation among various design alternatives in order to increase the crashworthiness of the electric car against a side post collision, only that of using aluminum foam as filler of the door sill structure gave a battery pack deformation that is acceptable, i.e. 9.4 mm compared to the 15.3 mm limit. Therefore, it can be concluded that a door sill structure filled with aluminum foam is safe to protect the battery pack against a side post collision in accordance with the Euro NCAP standard.

However, with an additional mass of 18.8 kg, it is unlikely to be implemented in a small city car. From the current study, it is advisable to optimize the design of either hollow pipes, aluminum honeycomb or aluminum foam in order to obtain effective impact energy absorption with low additional mass. With consideration of manufacturability and assembly, using aluminum hollow pipes or a honeycomb structure with the correct dimensions could provide the optimum solution to reach crashworthiness of the electric vehicle.

References

[1] Yoshio, M. & Noguchi, H., *A Review of Positive Electrode Materials for Lithium-Ion Batteries*, Lithium-ion Batteries: Science and Technologies, M. Yoshio, R.J. Brodd, & A. Kozawa (eds.), Springer, pp. 9-48, 2009.

[2] Kumar, R.V. & T Sarakonsri, *Introduction to Electrochemical Cells,* High Energy Density Lithium Batteries: Materials, Engineering, Applications, K.E. Aifantis, S.A. Hackney, & R.V. Kumar (eds.), Wiley-VCH, Weinheim, pp. 1-26, 2010.

[3] Greve, L. & Fehrenbach, C., *Mechanical Testing and Macro-Mechanical Finite Element Simulation of the Deformation, Fracture, and Short Circuit Initiation of Cylindrical Lithium Ion Battery Cells*, Journal of Power Sources, **214**, pp. 377-385, 2012.

[4] Woollaston, V., *New Blow for Tesla: Fire in the 'World's Safest Electric Car' Began in Vehicle's Battery*, Daily Mail, http://www.dailymail.co.uk/sciencetech/article-2442392/New-blow-

Tesla-Fire-worlds-safest-electric-car-began-vehicles-battery.html (accessed on 3 August 2015).
[5] Lyle, *Chevy Volt Powertrain*, http://gm-volt.com/2010/01/16/gm-to-open-electric-motor-plant/ (accessed on 22 July 2015).
[6] *Location of the Battery Pack Shown in a Cutaway of the 2013 Nissan Leaf Exhibited in Norway during the Launch of the New Year Model*, Norsk Elbilforening, https://www.flickr.com/photos/80208777@N05/8633427325 (accessed on 22 July 2015).
[7] The European New Car Assessment Programme (Euro NCAP), *Side Impact Mobile Deformable Barrier Testing Protocol v7.0.1. 2015,* http://euroncap.blob.core.windows.net/media/17003/euro-ncap-side-protocol-ae-mdb-v701-april-2015.pdf (accessed on 3 June 2015).
[8] The European New Car Assessment Programme (Euro NCAP), *Oblique Pole Side Impact Protocol v7.0.1. 2015,* http://euroncap.blob.core.windows.net/media/17002/euro-ncap-pole-protocol-oblique-impact-v701-april-2015.pdf (accessed on 3 June 2015).
[9] The European New Car Assessment Programme (Euro NCAP), *Adult Occupant Protection,* http://www.euroncap.com/en/vehicle-safety/the-ratings-explained/adult-occupant-protection/ (accessed on 8 August 2015).
[10] *Mitsubishi i-Miev, EV World*, http://evworld.com/press/mitsubishi_i-miev_battghost.jpg, (Accessed on 28 July 2015)
[11] Paik, J.K., Thayamballi, A.K. & Kim, G.S. *The Strength Characteristics of Aluminum Honeycomb Sandwich Panels,* Thin-Walled Structures, **35**(3), pp. 205-231, 1999.
[12] Yu, C.J. & J. Banhart, *Mechanical Properties of Metallic Foams*, Fraunhofer Proceeding of Fraunhofer USA Metal Foam Symp., Stanton, Delaware, October 1997, https://www.helmholtz-berlin.de/media/media/spezial/people/banhart/html/B-Conferences/b020_yu1998.pdf, 1998 (accessed on 28 July 2015).